

# Physical, Mechanical and Magnetic Properties of the Yb-Substituted $\text{Bi}_2\text{Sr}_2\text{Ca}_1\text{Cu}_2\text{O}_y$ Textured Superconductor

H. Gündoğmuş · B. Özçelik · B. Özkurt · A. Sotelo · M.A. Madre

Received: 10 May 2012 / Accepted: 2 July 2012 / Published online: 20 July 2012  
© Springer Science+Business Media, LLC 2012

**Abstract** In this study, samples with nominal composition of  $\text{Bi}_2\text{Sr}_2\text{Ca}_1\text{Cu}_{2-x}\text{Yb}_x\text{O}_y$ , where  $x = 0.0, 0.05, 0.1$  and  $0.25$ , have been textured using the Laser Floating Zone technique. The effects of different Yb doping on the structure have been investigated by electrical resistivity, scanning electron microscopy, XRD, mechanical and dc-magnetization techniques. It has been found that with increasing  $\text{Yb}^{3+}$  doping for Cu, the physical and superconducting properties of structure gradually decrease.  $J_C$  values, calculated using the Bean's model, significantly change, although  $T_C$  is approximately the same for all samples.

**Keywords** Bi-2212 · LFZ technique · XRD · Resistivity · Magnetic properties · Critical current

## 1 Introduction

Since the discovery of high-temperature superconductor, many substitution studies have been made on  $\text{HT}_C\text{-BSCCO}$  system in Cu sites to improve the physical and magnetic properties of the superconducting phase [1–4]. The effect of

substitution on the Cu sites is more important than on other ones since the transition temperatures in ceramic superconductors depend on the charge carrier concentration in the Cu–O planes. It is well known that holes in the Cu–O planes created by electron doping constitute an important parameter to achieve superconductivity. There are three well-known phases in the Bi-based superconductors with general formula  $\text{Bi}_2\text{Sr}_2\text{Ca}_{n-1}\text{Cu}_n\text{O}_y$  where  $n = 1, 2$ , and  $3$ . The transition temperatures of these different phases are related to the number of the Cu–O layers per unit cell.

In addition, the material preparation techniques for the BSCCO systems play a crucial role, as important as the substitutions which can be made in BSCCO. Moreover, this system possesses a high crystallographic anisotropy which can be exploited by an adequate grain alignment to produce high quality tapes and wires, as well as bulk materials with improved electrical properties. Laser Floating Zone (LFZ) melting technique is the one of best methods used to texture these bulk superconductor samples [5]. This method provides well aligned Bi-2212 grains, with their  $c$ -axis nearly perpendicular to the growth direction, and very small amount of secondary phases [6, 7].

In this work, the effect of the Yb substituting for Cu on the mechanical, physical and superconducting properties of samples prepared by using the LFZ method has been investigated. The prepared samples have been characterized using X-ray powder diffraction (XRD), electrical resistivity, scanning electron microscopy (SEM) and magnetic measurements. In addition, it is important to know how Yb addition affects the mechanical properties of the LFZ grown Bi-2212 materials. Thus, flexural strength tests have also been made to determine the mechanical behavior of samples.

H. Gündoğmuş (✉) · B. Özçelik  
Department of Physics, Faculty of Sciences and Letters,  
Çukurova University, 01330 Adana, Turkey  
e-mail: [hkgundogmus@gmail.com](mailto:hkgundogmus@gmail.com)

B. Özkurt  
Department of Electronic and Computer Education,  
Faculty of Tarsus Technical Education, University of Mersin,  
Mersin, Turkey

A. Sotelo · M.A. Madre  
ICMA (CSIC-Universidad de Zaragoza), María de Luna, 3,  
50018 Zaragoza, Spain

## 2 Experimental Details

$\text{Bi}_2\text{Sr}_2\text{CaCu}_{2-x}\text{Yb}_x\text{O}_y$  samples, with  $x = 0.0, 0.05, 0.1$  and  $0.25$  Yb additions, have been prepared from commercial  $\text{Bi}(\text{CH}_3\text{COO})_3$  ( $\geq 99.99\%$ , Aldrich),  $\text{Sr}(\text{CH}_3\text{COO})_2 \cdot \frac{1}{2}\text{H}_2\text{O}$  (99 %, Panreac),  $\text{Ca}(\text{CH}_3\text{COO})_2 \cdot \text{H}_2\text{O}$  (98 %, Alfa Aesar),  $\text{Cu}(\text{CH}_3\text{COO})_2 \cdot \text{H}_2\text{O}$  (98 %, Panreac), and  $\text{Yb}(\text{CH}_3\text{COO})_3 \cdot \text{H}_2\text{O}$  (99.9 %, Alfa Aesar) powders. They were dissolved in a mixture of glacial acetic acid (PA, Panreac) and distilled water. To the resulting clear light blue solution, polyethyleneimine (PEI) (Aldrich, 50 wt% water) was added and the solution turned dark blue immediately, indicating the polymer-cations coordination through the nitrogen atoms. After partial evaporation ( $\sim 80$  vol.%) of water and acetic acid in a rotary evaporator, the concentrated solution was placed on a hot plate at  $50^\circ\text{C}$  until a very dark blue thermoplastic paste appeared. Further heating produced a slow combustion with the release of brown fumes (nitrogen oxides), producing a very fine powder. This product was then milled in an agate mortar, and calcined twice, at  $750$  and  $800^\circ\text{C}$ , for 12 h with an intermediate manual milling. These pre-reacted powders were then used to prepare cylindrical precursors, approximately 120 mm long and 3 mm in diameter by cold isostatic pressing with an applied pressure of 200 MPa during 1 min. The green ceramic cylinders were subsequently used as feed in an LFZ melting installation described elsewhere [8]. Fibers were grown using a growth rate of 15 mm/h and a relative rotation of 18 rpm between the seed and feed. Using these growth conditions and adjusting the laser power input to obtain a molten zone of 1–1.5 times the rod diameter, it is possible to obtain a stable solidification front, which allows the fabrication of homogeneous textured bars.

Bi-2212 ceramics presents incongruent melting, and, in consequence, after the directional solidification process, it is necessary to perform a thermal treatment in order to form the Bi-2212 superconducting phase [9, 10]. This annealing process was performed under air, and consisted in two steps: 60 h at  $860^\circ\text{C}$ , followed by 12 h at  $800^\circ\text{C}$ , and, finally, quenched in air to room temperature.

Phase determination has been performed on annealed samples using X-ray powder diffraction measurements (Rigaku D/max-B) with  $2\theta$  ranging between  $10^\circ$  and  $80^\circ$ . Microstructural characterization was made on polished longitudinal cross sections of the samples, after the annealing process, in a scanning electron microscope (SEM, JEOL JSM 6400) equipped with an energy-dispersive spectroscopy (EDX) system. Electrical measurements were performed by the conventional four-point probe configuration on about 30 mm long samples. The magnetic measurements of samples were performed with a 7304 model LakeShore VSM at temperatures of 10 and 25 K and an applied field of  $\pm 1$  T. Finally, mechanical characterization

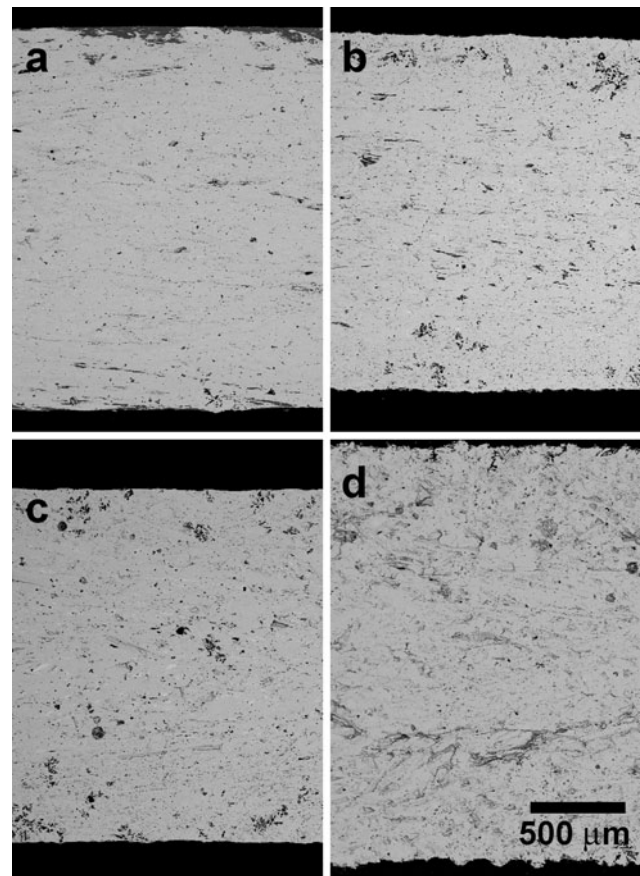


**Fig. 1** SEM micrographs of polished longitudinal sections of the Yb-doped Bi-2212 textured materials after annealing: (a)  $x = 0.0$ ; (b) 0.05; (c) 0.1; and (d) 0.25 Yb. Dark contrasts correspond to  $(\text{Sr,Ca})\text{CuO}_2$  secondary phases

has been performed by flexural strength, using the three-point bending test in an Instron 5565 machine with a 10-mm loading span fixture and a punch displacement speed of  $30\ \mu\text{m}/\text{min}$ .

## 3 Results and Discussion

After texturing processes all the bars have similar diameters, but after annealing an important change on the 0.25Yb-substituted samples has been observed. Their diameters increase from  $\sim 2.0$  to  $2.3$  mm while the other samples maintain very similar diameters before and after the annealing. This effect can be clearly observed in Fig. 1, where SEM images corresponding to longitudinal polished sections of samples after annealing are displayed. In this figure it can be seen that diameters of the samples are similar in all the cases, except for the 0.25Yb-substituted sample, for which the diameter is larger than for the rest of the samples. A careful observation indicates that the amount of secondary phases (mostly observed as dark contrasts, corresponding to the  $(\text{Sr,Ca})\text{CuO}_2$  secondary phase) increases when the amount of Yb is raised.

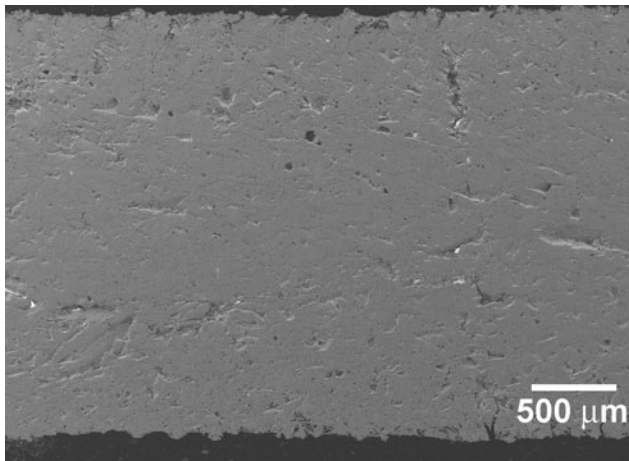


**Fig. 2** SEM micrographs of polished longitudinal sections of the 0.25Yb-doped Bi-2212 textured materials after annealing, taken with secondary electrons in order to observe porosity in the samples

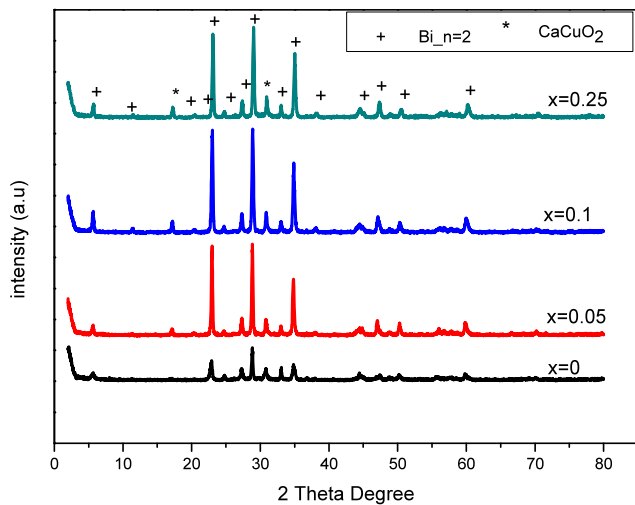


**Fig. 3** X-ray diffraction patterns of the  $\text{Bi}_2\text{Sr}_2\text{CaCu}_{2-x}\text{Yb}_x\text{O}_y$  superconducting samples. (+) Bi-2212 phase, and (\*)  $(\text{Sr,Ca})\text{CuO}_2$  secondary phases

In order to explain the different behavior of the 0.25Yb-substituted samples, secondary-electrons SEM micrographs have been recorded and a representative one is displayed in Fig. 2. In this figure it can be observed that these samples possess a high amount of porosity, which explains the increase of their diameters after annealing.

In order to identify the phases present in the samples, powder XRD has been performed on all the textured samples. The obtained patterns are displayed in Fig. 3. They show that main peaks (indicated by +) in all the samples correspond to the Bi-2212 phase, which clearly indicates that the performed thermal treatment is adequate to produce the superconducting phase as the major one. However, some minor peaks corresponding to the  $\text{CaCuO}_2$  phase (indicated by \*) have also been detected.

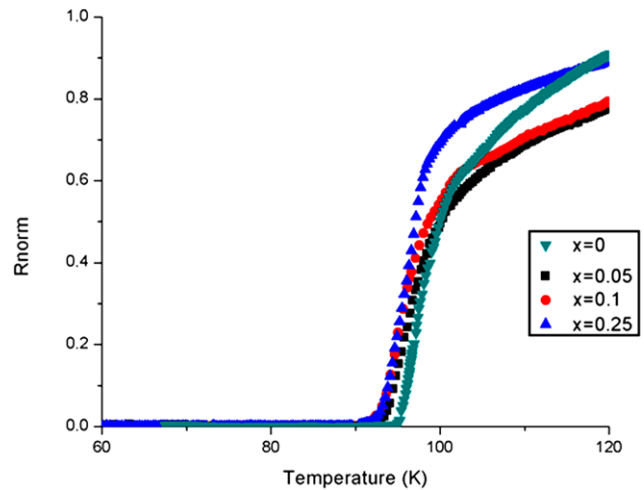


**Fig. 4** Resistivity measurement vs. temperature for all the samples

Figure 4 shows the temperature dependence of the resistivity. In this figure it is clear that  $T_C$  is similar for all the Yb-doped samples, but slightly lower than the one obtained for the undoped samples. On the other hand, for temperatures higher than the superconducting to normal state transition, all the samples show a metallic behavior. In addition, Table 1 shows that the width of  $\Delta T_C$  increases monotonically with the increase of Yb content in the samples. Nevertheless, these  $\Delta T_C$  changes remain quite small while Yb content increases, which indicates a single-phase transition ( $n = 2$ , Bi-2212) with a small degree of secondary phases.

The  $M-H$  hysteresis loops have been measured at different temperatures: 10, 15, 20 and 25 K. In Figs. 5 and 6 the results at 10 and 25 K, respectively, are presented for clarity, as the samples' evolution is the same in all the cases. All those  $M-H$  hysteresis loops were obtained after cooling the sample in zero magnetic field (ZFC) and measured between the applied external fields of  $\pm 10$  kOe. The hysteresis curves of samples performed at different temperatures demonstrate that the pure sample exhibits the largest area which decreases when Yb content is increased.

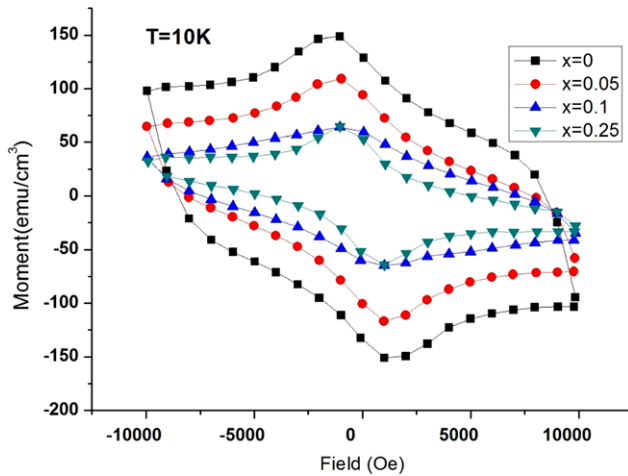
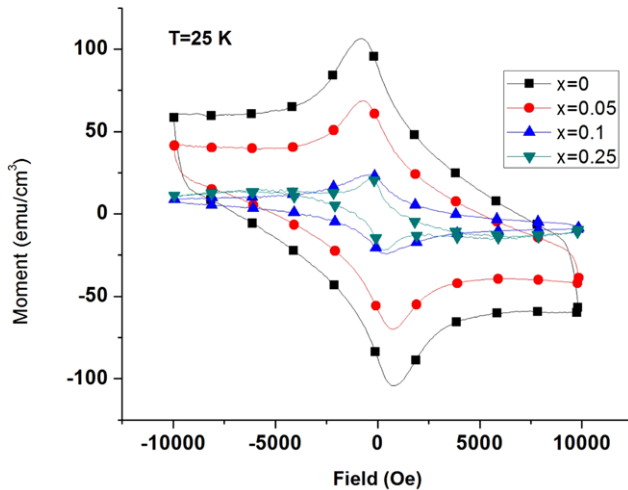
The  $J_C$  values of the samples were calculated from these data using the Bean's model [11]:

$$J_C = 30 \frac{\Delta M}{d}$$

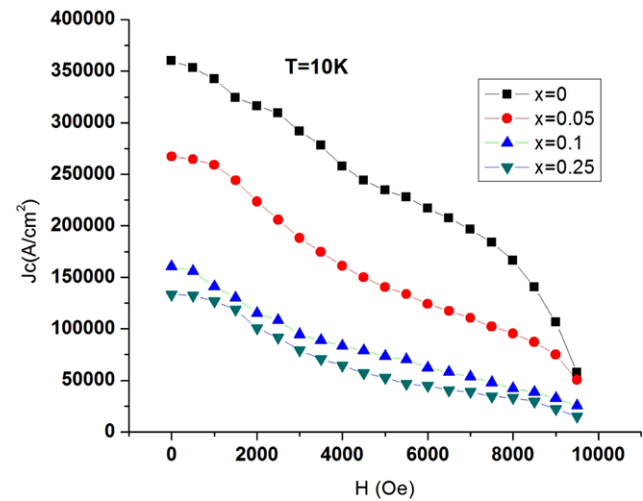
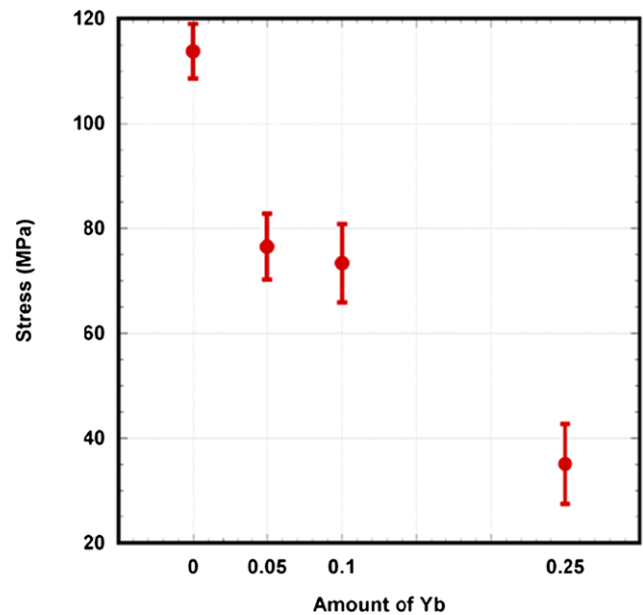
where  $J_C$  is the magnetization current density in amperes per square centimeter,  $\Delta M = M_+ - M_-$  is measured in electromagnetic units per cubic centimeter,  $d$  is the thickness of the sample. Figure 7 shows the calculated critical current densities as a function of the applied field for all the samples, at  $T = 10$  K.  $J_C$  calculations reveal that the pure sample exhibits better superconducting properties and has the biggest  $J_C$  values. These results indicate that  $J_C$  values significantly decrease when magnetic field is raised and the amount of Yb is increased.

**Table 1** Resistivity measurement results for the samples

Samples	$T_C^{\text{onset}}$ (K)	$T_C^{\text{offset}}$ (K)	$\Delta T_C$ (K)
$x = 0$	100	95	5
$x = 0.05$	98.57	93.21	5.36
$x = 0.1$	97.71	92.05	5.66
$x = 0.25$	98.46	92.27	6.19

**Fig. 5**  $M$ – $H$  hysteresis loops of samples at  $T = 10$  K and applied external fields of  $\pm 10$  kOe**Fig. 6**  $M$ – $H$  hysteresis loops of samples at  $T = 25$  K and applied external fields of  $\pm 10$  kOe

In addition to the above measurements, the mechanical behavior of the samples has been studied by three-point bending tests. The mean mechanical stress, together with its standard error bars, is represented in Fig. 8 for the different samples. From this figure it is clear that while Yb values increase, the mechanical stress decreases due to the formation of secondary phases and the decrease on the grain orientation (see Fig. 1). Moreover, the mechanical stress de-

**Fig. 7** Calculated  $J_C$  results of samples at  $T = 10$  K from their hysteresis loops**Fig. 8** Mean maximum mechanical stress (three-point flexure strength), together with their standard error, as a function of Yb amount

creases dramatically for 0.25Yb-substituted samples due to the formation of a high amount of internal porosity (see Fig. 2).

## 4 Conclusions

In the present study,  $\text{Bi}_2\text{Sr}_2\text{CaCu}_{2-x}\text{Yb}_x\text{O}_y$  ( $x = 0.0, 0.05, 0.1$  and  $0.25$ ) samples were successfully textured using the LFZ method. Resistivity results pointed out that the  $T_C$  of the samples slightly changes with the increase of Yb concentration. From XRD patterns, it has been found that the Bi-2212 phase is the major one in all the samples. Magnetic hysteresis and calculated  $J_C$  values show that the magnetic properties and critical current values of the samples decrease with increasing of the substitution level. Mechanical stress is found to be highly sensitive to the doping level as it decreases when Yb content increases.

**Acknowledgements** This work is supported by the Research Fund of Cukurova University, Adana, Turkey, under grant contracts No. FEF 2011D21. The Spanish MICINN-FEDER (Project MAT2008-00429) and the Gobierno de Aragón (Consolidated Research Group T12) are acknowledged for financial support.

## References

1. Chattopadhyay, B., Bandyopadhyay, B., Poddar, A., Mandal, P., Das, A.N., Ghosh, B.: *Physica C* **331**, 38 (2000)
2. Ilonca, G., Toma, V., Yang, T.R., Pop, A.V., Balint, P., Bodea, M., Macocian, E.: *Physica C* **460–462**, 369 (2007)
3. Wang, X.L., Horvat, J., Gu, G.D., Uprety, K.K., Liu, H.K., Dou, S.X.: *Physica C* **337**, 221 (2000)
4. Yamamoto, T., Kakeya, I., Kadowaki, K.: *Physica C* **460–462**, 799 (2007)
5. Sotelo, A., Mora, M., Madre, M.A., Diez, J.C., Angurel, L.A., De la Fuente, G.F.: *J. Eur. Ceram. Soc.* **25**, 2947–2950 (2005)
6. Madre, M.A., Amaveda, H., Mora, M., Sotelo, A., Angurel, L.A., Diez, J.C.: *Bol. Soc. Esp. Cerám. Vidr.* **47**(3), 148–152 (2008)
7. Angurel, L.A., Diez, J.C., Martínez, E., Peña, J.I., De la Fuente, G.F., Navarro, R.: *Physica C* **302**(1), 39–50 (1998)
8. Carrasco, M.F., Costa, F.M., Silva, R.F., Gimeno, F., Sotelo, A., Mora, M., Diez, J.C., Angurel, L.A.: *Physica C* **415**, 163 (2004)
9. Funahashi, R., Matsubara, I., Ueno, K., Ishikawa, H.: *Physica C* **311**, 107 (1999)
10. Mora, M., Martínez, E., Diez, J.C., Angurel, L.A., De la Fuente, G.F.: *J. Mater. Res.* **15**, 614 (2000)
11. Bean, C.P.: *Phys. Rev. Lett.* **8**, 250 (1962)